ACTA METALLURGICA SLOVACA
2022, VOL. 28, NO. 1, 19-24

RESEARCH PAPER

METALLURGICAL AND MECHANICAL INVESTIGATION OF TIG ARC WELDMENTS FOR API X60 STEEL PIPES

*Taher El-Bitar[1], Maha El-Meligy[1], Mohammed Gamil[2]**

[1]Plastic Deformation Department, Central Metallurgical R&D Institute (CMRDI), Cairo 11422, Egypt
[2]Department of Mechanical Engineering, Faculty of Engineering at Shoubra, Benha University, Cairo 11629, Egypt

*Corresponding author: mohammed.gamil@feng.bu.edu.eg, tel.: +201004635264, Faculty of Engineering at Shoubra / Benha University, 11629, Cairo, Egypt

Received: 13.12.2021
Accepted: 01.02.2022

ABSTRACT

API steel gas pipe of 812.8 mm diameter and 15.9 mm wall thickness was investigated to characterize the steel grade and assess weldability for fourteen-consecutive passes of TIG arc welding technology. The parent Metal (PM) contains 0.02% C in addition to 0.02% Nb. A steel electrode for TIG process was used containing 5.6% Cr and 0.56% Mo. Standard V-groove was mechanically prepared to suite butt welding. The microstructure of the PM was containing mainly fine acicular ferrite satisfying the essential requirements of API specifications for grade X60. The weld metal (WM) was containing very fine acicular ferrite and showing the maximum hardiness values. Heat affected zone (HAZ) structure still contains acicular ferrite but it became coarse, possessing lower hardness than that of WM. HAZ does not exceed 2-2.5 mm adjacent to the welded V-groove. The fractured tensile welded specimens were necked and failed at the HAZ. The impact transition temperature (ITT) was detected as -35 °C. However, the mechanical properties of the WM did not negatively affected by the welding process and still fair satisfying the requirements of API X60.

Keywords: steel pipes; Weldability; Tungsten inert gas (TIG); Acicular ferrite; Impact transition temperature (ITT).

INTRODUCTION

Exploration of gas and oil is accompanied by extensive development of steel pipe processing for transportation purposes from wells for refining and storing places. Efforts have been directed towards enhancement of steel properties to cope with the API specifications [1]. Enhancement is dealing with the tensile properties as well as the impact toughness even at lower temperatures. Special attention was paid to the micro-alloying elements; in addition to thermo-mechanical treatment during the steel processing. Weldability of steel and welding technologies are highly concerned.

Recently, low carbon micro-alloyed steels are developed through microstructure refinement to improve both strength and toughness. Great attention has been taken to attain ultra-fine ferrite grain structure for creation strain induced ferritic transformation (acicular ferrite) and/or dynamic recrystallization of austenite during deformation [2, 3]. However, for pipeline steel, acicular ferrite microstructure is favorable, as it would have better properties such as high tensile strength, good toughness, excellent corrosion resistance and superior weldability [4-6]. The previous properties were leading to the application of the acicular ferrite steel plates in the manufacturing of large diameters pipes for gas and oil transportation at the low temperature areas [7, 8].

Microalloying elements such as Nb, V and Ti have a controlling influence on the recrystallization behavior of austenite in steel, either while in solid solution or as second phase precipitates. Microalloying affects the critical temperature for onset of grain coarsening during reheating and subsequent hot deformation [9]. The principal advantage of the micro-alloyed steels is not only their good combination of strength and toughness, but also their good weldability [10, 11]. Large diameter API steel pipes demand WM with superior properties i.e., a combination of high strength and high toughness. These properties are usually secured by both micro-alloying [12] and a thermo- mechanical processing during steel processing for acicular ferrite creation to secure the high strength in combination with high toughness [13].

An important and essential requirement for weldability at the API specification is the carbon equivalent (CE) term which, was formulated by the International Institute of Welding (IIW) [14], as stated in equation (1).

$$CE = C + \frac{\%Mn}{6} + \frac{\%Cr + \%Mo + \%V}{5} + \frac{\%Ni + \%Cu}{15} \quad (1.)$$

Weldability is a complex concept, which depends on different factors. Chemical composition is important factor, in addition to steel processing route, welding technology applied, temperature, air humidity, and wind intensity in an open air [15]. Low CE steels were assessed as high weldability steels. However, susceptibility for occurrence of cracks, or other failures in the welded joint, or at the HAZ are also important to consider. Therefore, it is important to mention that the CE is only an indicative parameter for assessing the weldability and should never be based on its values to ensure the integrity of the welded joints [15].

However when high strength steel is welded, care would be taken, where non-uniform heating and cooling in WM and parent metal generating harder HAZ, cold crack susceptibility and residual stress in weldments [13]. On the bases of a previous

work, it was stated that in the high API steel grades (≥ X60), the HAZ is prone to failure due to the possibility of hydrogen induced cracking and the only way to weld such steels is to use low hydrogen ferritic steel filler wire [16]. The WM microstructure of fusion welded joints is greatly influenced by both chemical composition of filler metal and the heat input of the process. High heat input is leading to longer time for cooling which results in coarse grains in WM. On the other hand, lower heat input leads to fast cooling which results in fine microstructure [17].
It was found that in gas metal arc welding of HSLA naval grade steel joints that the parent metal microstructure contained mainly ferrite and few amount of pearlite. The microstructure was transformed into acicular ferrite, little amount of retained austenite and martensite as a result of heat input and chemical composition [13]. A previous study stated that microstructural stability is more in acicular ferrite compared to bainite in higher temperatures [18].
The current work aims at investigation the metallurgical and mechanical characterization of API 812.8 mm diameter gas pipe. Weldability assessment for TIG arc welding process is also investigated. Not only CE but also experimental measurements for mechanical properties and metallographic characteristics of the welded joints are used.

MATERIAL AND METHODS

The parent metal (PM) under investigation is a steel sample pipe, with 812.8 mm diameter and 15.9 mm wall thickness. For the steel alloy characterization; chemical analysis as well as tensile, impact, and bending specimens were mechanically cut and suitable tests have been carried out. Steel plates were prepared for TIG welding process as V- grooves by milling in accordance with ISO 9692. The V- grooves dimensions are shown in **Fig. 1**.
Fig. 2 presents schematically the sequence of 14 - consecutive TIG welding passes for filling the V-grooves of the steel plates
The used consumed electrodes of the TIG welding process have 2.4 mm diameter. The electrodes were selected as low-carbon steel alloys containing Cr and Mo, which is complying with ER80S-B6 according to AWSA5.28. **Table 1** states the chemical composition of the used consumable ER80S-B6 electrodes.

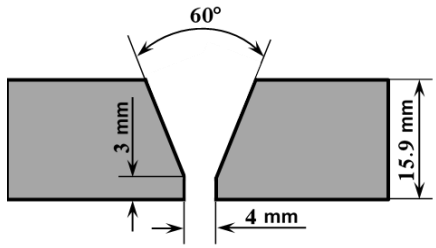

Fig. 1 V-groove for butt welding from one side according to ISO 9692

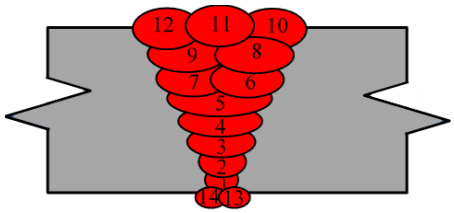

Fig. 2 Schematic illustration of 14 - consecutive TIG Welding passes

Table 1 Chemical composition of the consumable electrode (wt.%)

C	Si	Mn	Cr	Ni	Mo	Cu	P	S	Fe
0.07	0.49	0.51	5.62	0.1	0.56	0.04	0.01	0.009	Balance

The standard mechanical properties of the consumed electrodes are 500 MPa yield strength, 620 MPa ultimate tensile strength and 20% elongation. The electrode-negative polarity was applied to achieve the benefits of faster melt-off and faster deposition rate. The applied current was 140 A and the argon flow rate was maintained 8 L/min, during the whole welding process. **Fig. 3** presents a macrograph for the 14-consecutive butt welding passes. Locations of 17-indentations of the Hardness Vickers testes are also presented in **Fig. 3**.
Table 2 states the duration of each welding pass and the total and average welding time per pass in seconds for filling the v-groove by TIG process.

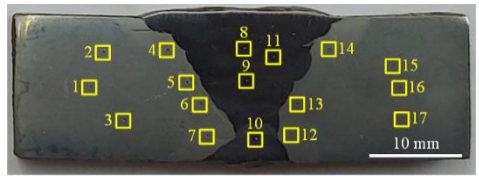

Fig. 3 Presentation of the 14-consecutive passes of TIG welding process and 17 - locations of hardness indentions

Suitable hardness, tensile, impact, and bending test specimens were mechanically prepared, where the welding zone is passing at the middle of the test specimens as schematically presented in **Figs. 3, 4**.
Hardness tests were executed using 10 Kgf and 15 sec. dwell time on the PM, HAZ, weld metal (WM), complying with DIN 501333. Tensile tests were carried out according to the specs of DIN 50125, while the impact tests were done at room temperature as well as at lower temperatures up to -65 ^{o}C in accordance with DIN standard EN100045. Furthermore, bending tests was carried out in accordance with the requirements of DIN 50111. Suitable specimens were prepared from different zones for microstructure investigations.

RESULTS AND DISCUSSION

The chemical composition of the PM for the sample pipe is stated in **Table 3**. It is clearly noticed that the pipe is a steel containing 0.022% carbon, which is lower than the maximum amount permitted of carbon (0.22%) in the API 5L PSL2 specifications. Furthermore, the steel contains 1.65 % Mn, which satisfies the requirements of API steel grades. The harmful elements, P and S are lower than 0.025 % and 0.015 % respectively. At the same time, the sum of Nb, V and Ti reaches to 0.035% in the steel sample, while the API specifications stipulate to be less than 0.15%.
The calculated CE value, according to equation (1), reaches to 0.3 wt.% which is less than 0.43 wt.% as declared in API 5L PSL2 specifications [1]. The PM can be assisted as high weldability steel, where CE is only an indicative parameter for assessing weldability [15].
Fig. 5 presents fine grained ferritic microstructure of the PM as a result of low carbon contents and micro-alloying with Nb.

Table 2 Welding times for each pass and average welding time in seconds

Pass No.	1	2	3	4	5	6	7	8	9	10	11	12	13	14	Total	Average
Welding time, Sec.	122	87	94	87	101	100	69	94	73	118	93	114	66	48	1266	90.43

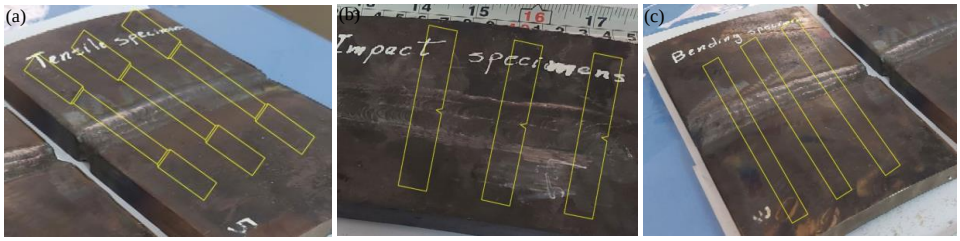

Fig. 4 Locations of tensile, impact, and bending test specimens taken after butt TIG arc welding process (a) Tensile test specimens, (b) Impact test specimens (c) Bending test specimens

Table 3 Chemical composition of the PM (wt.%)

C	Si	Mn	Cr	Ni	Mo	Cu	P	S	Nb	Ti	V	Al	Fe
0.022	0.337	1.65	0.017	0.009	0.001	0.002	0.015	0.004	0.022	0.009	0.006	0.04	Balance

Fig. 5 Micrograph of fine grained ferritic microstructure

Round longitudinal tensile test specimens were taken, where the thickness of the pipe is greater than 12.7 mm as in indicated the API specifications. **Table 4** compares the actual tensile results of PM of the sample pipe with that of the standard API X60. It is clear that the yield stress as well as the ultimate strength and elongation results satisfy the requirements of API steel grade X60.

High magnified microstructure on a prepared surface of the PM (**Fig. 6a**) reveals deformation induced ferrite (acicular ferrite) [15]. **Fig. 6b** shows the Energy-dispersive X-ray (EDX) chart, which ensures speared of acicular ferrite in the matrix. Transformation to acicular ferrite explains the extremely high values of the tensile properties presented on **Table 4** despite of containing 0.02 % carbon content of steel. Speared of acicular ferrite in the steel matrix assured the use of thermo-mechanical processing technology by consecutive hot rolling passes followed by early cooling on the run out table (ROT) [12]. Acicular ferrite microstructure has the potential of combining high strength and high toughness [9].

The measured impact toughness on the specimens of parent metal at 0 °C reaches to a value higher than 300 J (Maximum capacity of impact test machine) satisfying the essential requirement of API 5L PSL2 standard for grade X60. **Fig. 7** shows the different impact specimens, where they are not separated fractured after impact testing, but only bended.

Table 4 Tensile properties of the sample pipe compared with standard API X60 steel grade

Properties	Yield stress at 0.2% FS (MPa)	Ultimate strength (MPa)	Elongation (%)
Sample pipe	498.56	578.99	24.07
Standard API X60	414-565	517-758	17

The second phase of the current work is dealing with the weldability assessment for joints on the PM. Hardness measurements can be a quick and accurate tool for assessing the effect of the welding process on the properties of the PM. **Fig. 8** presents the hardness distribution profile around the welding axis. It is clearly noticed that hardness reaches maximum at the WM at the welding axis, after which hardness becomes lower at the HAZ, which does not exceed 2-2.5 mm adjacent to the WM. The PM possesses hardness values higher than that at HAZ. The consumed electrode contains 5.62 % Cr in addition to 0.56% Mo as stated in **Table 1**. Both alloying elements were intentionally added to the electrode alloy for enhancing the hardenability of the WM [19]. Reference [19] emphasizes that alloying Cr with 0.5% Mo is almost completely suppressing the formation of polygonal ferrite even at a slow cooling rate of 0.5 °C/s. High hardness in the WM is also attributed to the fine grain size and needle-shape of the formed acicular ferrite. The steep hardness gradient within the WM is attributed to the uncontrolled open atmospheric cooling rate and the grain size gradient from the welding line [18].

Fig. 9 presents high magnified microstructure of the WM. The micrograph contains very fine acicular ferrite. Suppressing of polygonal ferrite formation is pronounced as a result of containing Cr and Mo [19].

The total duration of 14-consecutive welding passes (**Table 2**) was reaching to 1266 sec, with 90.43 sec average welding time for each pass. It is considered as long time heating of the WZ resulting in a high amount of heat input to the HAZ. Consequently, hardness at the HAZ became low even less than hardness of the PM [17]. After the HAZ area, heat input has not a pronounced effect on the PM [20]. **Fig. 10** presents the microstructure of the HAZ and shows the negative effects of long time

heat input by welding passes [17-20], where the structure still acicular but became coarse with lower mechanical properties.

Tensile testing is the most common and effective mechanical test. Usually, the tensile properties of welded specimens reflect cumulative effects of different zones in the specimens. **Table 5** compares the results of the tensile properties between the PM and welded specimens. The table shows that both electrode chemical composition and heat input by welding has minor effects on the yield as well as ultimate strength, while the heat input by the welding passes has a pronounced effect on enhancing the elongation of welded test specimens [17-20].

The fractured tensile specimens were necked and followed by failing at the HAZ. **Fig. 11** presents photos of the failed tensile specimens, where failure was happened at the HAZ.

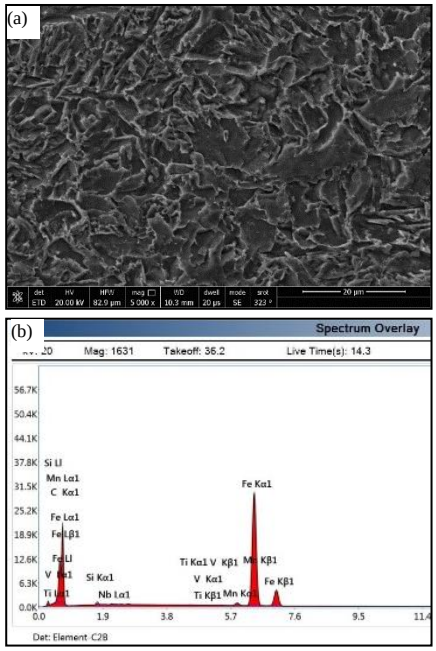

Fig. 6 High magnification microstructure and energy-dispersive X-ray (EDX) analysis of the PM, (a) High magnification microstructure of the PM, (b) Energy-dispersive X-ray (EDX) chart

Fig. 7 Impact toughness specimens of the PM after testing at 0 °C

Impact tests were performed at room as well as lower temperatures for the development of fracture criteria for the API steel weldment used in cold weather areas. The ductile to-brittle transition behaviour of a shielded metal-arc weld has been studied by measuring Charpy V-notch (CVN) impact energy. The CVN impact energy as a function of test temperature is shown in **Fig. 12**. The specimens have considerable impact values between 275 J at room temperature and 235 J at – 20 ºC. The WM exhibits then a gradual ductile-to-brittle transition with a transition temperature range extending from -20 °C to -50 °C [21]. A pronounced ITT is found at -35 ºC. The gradual change is observed on the amount of brittle facet structure, as shown in **Fig. 14**.

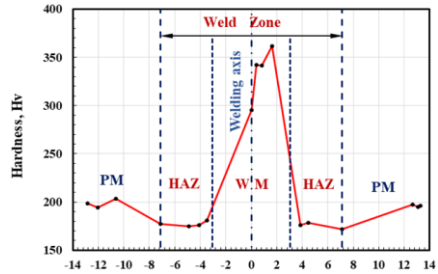

Fig. 8 Vickers hardness of the welded joints at the PM, HAZ and WM

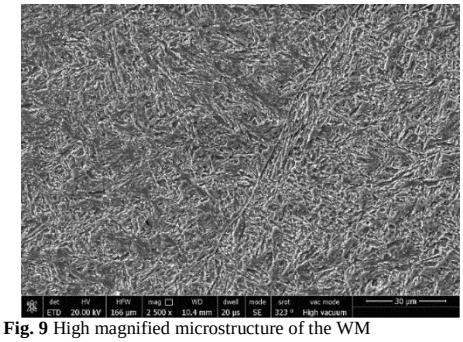

Fig. 9 High magnified microstructure of the WM

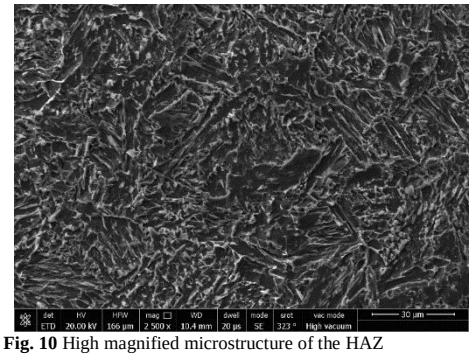

Fig. 10 High magnified microstructure of the HAZ

A representative fractograph of the impact specimens after testing at the room temperature is presented in **Fig. 13**. The fracture surface contains fully dimple structure indicating ductile fracture.

However, the fracture surface of impact specimens tested at -35 °C was changed completely to facets indicting brittle structure due to ITT from ductile to brittle as shown in **Fig. 14** [21-23].

Bending is a good and quick test for assessing the quality of the weldments. **Fig. 15** represents a photo of a welded specimen, which was bent to 180º around the weld face. It is clear that the bended specimen is completely sound indicating high quality welding process.

Table 5 Tensile properties of both PM and welded specimens

Sample Type	Yield Strength at 0.2% FS (MPa)	Ultimate tensile strength (MPa)	Elongation (%)
PM	498.56	578.98	24.06
Welded specimens	526.03	577.19	30.37

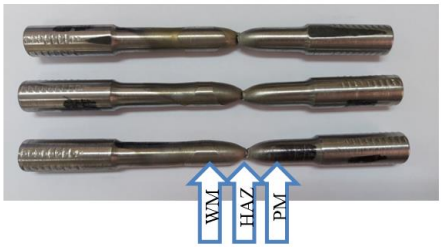

Fig. 11 Photo of the failed tensile specimens

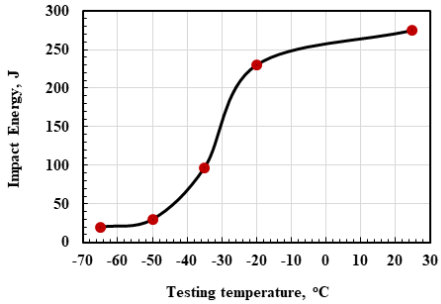

Fig. 12 Impact test results at different testing temperatures for the welded joints

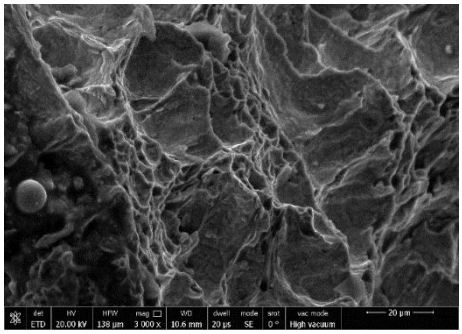

Fig. 13 Fracture surface of impact specimen tested at room temperature

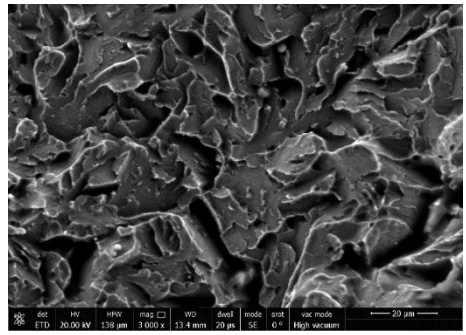

Fig. 14 Fracture surface of impact specimen tested at – 35 °C

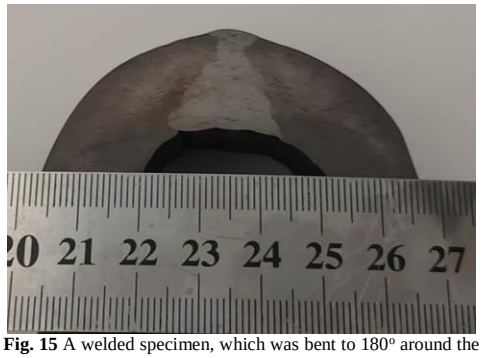

Fig. 15 A welded specimen, which was bent to 180° around the weld face

CONCLUSION

- The microstructure of the PM of the steel pipe contains mainly fine acicular ferrite.
- The PM was satisfying the essential requirements of API specifications for grade X60.
- The WM was containing very fine acicular ferrite and showing the maximum hardness values.
- HAZ structure still acicular but became coarse, possessing lower hardness than that of WM.
- HAZ does not exceed 2-2.5 mm adjacent to the welded V-groove.
- The fractured tensile welded specimens were necked and failed at the HAZ.
- ITT was detected as -35 °C.

Acknowledgments: Authors are grateful for the generous financial and technical support of CMRDI and Faculty of Engineering at Shoubra, Benha University, Egypt for carrying out this study.

REFERENCES

1. Specification for line pipe - API specification 5L, forty-third edition, march 2004. https://law.resource.org/pub/us/cfr/ibr/002/api.5l.2004.pdf (Accessed 13.12.2021).
2. H. Beladi, G. Kelly, A. Shokouhi, P. Hodgson: Materials Science and Engineering A, 371 (1-2), 2004, 343-352. https://doi.org/10.1016/j.msea.2003.12.024.
3. M. Jahazi, B. Egbali: Journal of materials processing technology, 103 (2), 2000, 276-279. https://doi.org/10.1016/S0924-0136(00)00474-X.

4. Y. Kim, S. Kim, Y. Lim, N. Kim: ISIJ international, 42(12), 2002, 1571-1577. https://doi.org/10.2355/isijinternational.42.1571.
5. YE. Smith, AP. Coldren, RL. Cryderman: Climax Molybdenum Company (Japan) Ltd., Tokyo, 1972, 119–142.
6. M.-C. Zhao, Y.-Y. Shan, F. R. Xiao, K. Yang, Y. H. Li: Materials Letters, 57 (1), 2002, 141-145. https://doi.org/10.1016/S0167-577X(02)00720-6.
7. K. Y. Y. Wang, Y. Shan, M. Zhao, B. Qian: The research and development of high strength line pipe in China, In.: *Proceedings of the International Pipe Dreamer's Conference*, Yokohama, Japan, 53–84, 2002.
8. T. Janzen, W.N. Horner: The Alliance Pipeline – A Design Shift in Long Distance Gas Transmission, In.: *Proceedings of ASME International Pipeline Conference (IPC)*, Alberta, Canada, 83-88, 1998.
9. R. Datta, S. Mishra: Bulletin of Materials Science, 17 (6), 1994, 643-662. https://doi.org/10.1007/BF02757548.
10. E. J. Czyryca, R. E. Link, R. J. Wong, D. A. Aylor, T. W. Montem, J. P. Gudas: Naval engineers journal, 102 (3), 1990, 63-82. https://doi.org/10.1111/j.1559-3584.1990.tb02632.x.
11. T. Montemarano, B. Sack, J. Gudas, M. Vassilaros, H. Vanderveldt: Journal of Ship Production, 2(03), 1986, 145-162. https://doi.org/10.5957/jsp.1986.2.3.145.
12. G. Megahed, S. Paul, T. El-Bitar, F. Ibrahim: Materials Science Forum, 500, 2005, 261-268. https://doi.org/10.4028/www.scientific.net/MSF.500-501.261.
13. S. R. Nathan, V. Balasubramanian, S. Malarvizhi, A. Rao: Defence Technology, 11 (3), 2015, 308-317. https://doi.org/10.1016/j.dt.2015.06.001.
14. T. Kasuya, N. Yurioka: Welding Journal, 72, 1993, 263-s - 268-s.
15. M. Rr, H. Osmani, M. Rama: Machines, Technologies, Materials, 10 (11), 2016, 40-43.
16. G. Magudeeswaran, V. Balasubramanian, G. M. Reddy, T. Balasubramanian: Journal of Iron and Steel Research International, 15(6), 2008, 87-94. https://doi.org/10.1016/S1006-706X(08)60273-3.
17. Y.-q. Zhang, H.-q. Zhang, J.-F. Li, W.-m. Liu: Journal of Iron and Steel Research International, 16(5), 2009, 73-80. https://doi.org/10.1016/S1006-706X(10)60014-3.
18. X. Wan, R. Wei, K. Wu: Materials Characterization, 61 (7), 2010, 726-731. https://doi.org/10.1016/j.matchar.2010.04.004.
19. F. Han, B. Hwang, D.-W. Suh, Z. Wang, D. L. Lee, S.-J. Kim: Metals and materials international, 14 (6), 2008, 667-672. https://doi.org/10.3365/met.mat.2008.12.667.
20. C. H. Suh, R. G. Lee, S. K. Oh, Y.-C. Jung, J.-Y. Son, Y. S. Kim: Journal of mechanical science and technology, 25 (7), 2011, 1727-1735. https://doi.org/10.1007/s12206-011-0424-x.
21. F. Zia-Ebrahimi: Ductile-to-brittle transition in steel weldments for arctic structures, National Bureau of Standards, U.S. Department of Commerce, Boulder, Colorado 80303, 1985. https://nvlpubs.nist.gov/nistpubs/Legacy/IR/nbsir85-3020.pdf (Accessed 13.12.2021).
22. T. El-Bitar, M. Gamil, I. Mousa, F. Helmy: Materials Science and Engineering: A 528 (18), 2011, 6039-6044. https://doi.org/10.1016/j.msea.2011.04.071.
23. A. Ray, S. Sivaprasad and D. Chakrabarti, International journal of fracture 173 (2), 215-222 (2012). https://doi.org/10.1007/s10704-012-9676-4.